

# Point defect engineered Si sub-bandgap light-emitting diode

Jiming Bao<sup>1</sup>, Malek Tabbal<sup>1,2</sup>, Taegon Kim<sup>1</sup>, Supakit Charnvanichborikarn<sup>3</sup>,  
James S. Williams<sup>3</sup>, Michael J. Aziz<sup>1\*</sup> and Federico Capasso<sup>1\*</sup>

<sup>1</sup>School of Engineering and Applied Sciences, Harvard University  
Cambridge, MA, 02138

<sup>2</sup>Department of Physics, American University of Beirut, Riad El Solh  
Beirut, 1107 2020, Lebanon

<sup>3</sup>Research School of Physical Sciences and Engineering, Australian National University, Canberra, Australia, 0200

\*Corresponding authors: [maziz@harvard.edu](mailto:maziz@harvard.edu), [capasso@deas.harvard.edu](mailto:capasso@deas.harvard.edu)

**Abstract:** We present a novel approach to enhance light emission in Si and demonstrate a sub-bandgap light emitting diode based on the introduction of point defects that enhance the radiative recombination rate. Ion implantation, pulsed laser melting and rapid thermal annealing were used to create a diode containing a self-interstitial-rich optically active region from which the zero-phonon emission line at 1218 nm originates.

©2007 Optical Society of America

**OCIS codes:** (230.3670) Light-emitting diodes; (160.6000) Semiconductors; (130-0250) Optoelectronics.

---

## References and links

1. S. Ossicini, L. Pavesi, and F. Priolo, *Light Emitting Si for Microphotonics*, Springer Tracts in Modern Physics Vol. **194**. (Springer-Verlag, Berlin, 2003).
2. K. D. Hirschman, L. Tsybeskov, S. P. Duttagupta and P. M. Fauchet, "Si-based visible light-emitting devices integrated into microelectronic circuits," *Nature* **384**, 338 (1996).
3. L. Pavesi, L. Dal Negro, C. Mazzoleni, G. Franzo and F. Priolo, "Optical gain in Si nanocrystals," *Nature* **408**, 440-444 (2000).
4. Z. Lu, D. J. Lockwood and J. Baribeau, "Quantum confinement and light emission in SiO<sub>2</sub>/Si superlattices," *Nature* **378**, 258-260 (1995).
5. A. G. Cullis and L. T. Canham, "Visible light emission due to quantum size effects in highly porous crystalline Si," *Nature* **353**, 335-338 (1991).
6. W. L. Ng, M. A. Lourenco, R. M. Gwilliam, S. Ledain, G. Shao and K. P. Homewood, "An efficient room-temperature Si-based light-emitting diode," *Nature* **410**, 192-194 (2001).
7. E. Ö. Sveinbjörnsson and J. Weber, "Room temperature electroluminescence from dislocation-rich silicon," *Appl. Phys. Lett.* **69**, 2686-2688 (1996).
8. P. L. Bradfield, T. G. Brown and D. G. Hall, "Electroluminescence from sulfur impurities in a p-n junction formed in epitaxial silicon," *Appl. Phys. Lett.* **55**, 100-102 (1989).
9. B. Zheng, J. Michel, F. Y. G. Ren, L. C. Kimerling, D. C. Jacobson and J. M. Poate, "Room-temperature sharp line electroluminescence at  $\lambda = 1.54 \mu\text{m}$  from an erbium-doped Si light-emitting diode," *Appl. Phys. Lett.* **64**, 2842-2844 (1994).
10. D. Leong, M. Harry, K. J. Reeson and K. P. Homewood, "A silicon/iron-disilicide light-emitting diode operating at a wavelength of  $1.5 \mu\text{m}$ ," *Nature* **387**, 686-688 (1997).
11. S. G. Cloutier, P. A. Kosyrev and J. Xu, "Optical gain and stimulated emission in periodic nanopatterned crystalline Si," *Nat. Mater.* **4**, 887-891 (2005).
12. H. Rong, A. Liu, R. Jones, O. Cohen, D. Hak, R. Nicolaescu, A. Fang and M. Paniccia, "An all-Si Raman laser," *Nature* **433**, 292-294 (2005).
13. O. Boyraz and B. Jalali, "Demonstration of a Si Raman laser," *Opt. Express* **12**, 5269 (2004).
14. M. S. Skolnick, A. G. Cullis and H. C. Webber, "Defect photoluminescence from pulsed-laser-annealed ion-implanted Si," *Appl. Phys. Lett.* **38**, 464-466 (1981).
15. G. Götz, R. Nebelung, D. Stock and W. Ziegler, "Photoluminescence investigation of defects after ion-implantation and laser annealing," *Nuclear Instruments and methods in physics research* **B2**, 757-760 (1984).

16. G. Davies, "The optical properties of luminescence centers in Si," *Phys. Rep.* **176**, 83-188 (1989).
17. S. Coffa, S. Libertino and C. Spinella, "Transition from small interstitial clusters to extended {311} defects in ion-implanted Si," *Appl. Phys. Lett.* **76**, 321-323 (2000); P.K. Giri, S. Coffa, and E. Rimini, "Evidence for small interstitial clusters as the origin of photoluminescence W band in ion-implanted Si," *Appl. Phys. Lett.* **78**, 291-293 (2001).
18. P.K. Giri, "Photoluminescence signature of Si interstitial cluster evolution from compact to extended structures in ion-implanted Si," *Semiconductor science and technology* **20**, 638-644 (2005).
19. P. J. Schultz, T. D. Thompson and R. G. Elliman, "Activation energy for the photoluminescence W center in Si," *Appl. Phys. Lett.* **60**, 59-61 (1992).
20. M. Nakamura, S. Nagai, Y. Aoki and H. Naramoto, "Oxygen participation in the formation of the photoluminescence W center and the center's origin in ion-implanted Si crystals," *Appl. Phys. Lett.* **72**, 1347-1349 (1998).
21. G. M. Lopez and V. Fiorentini, "Structure, energetics and extrinsic levels of small self-interstitials clusters in Si," *Phys. Rev. B*, **69**, 155206-155213 (2004).
22. C. R. Jones, J. Coutinho and P. R. Briddon, "Density-functional study of small interstitial clusters in Si: Comparison with experiments," *Phys. Rev. B* **72**, 155208-155212 (2005).
23. D. E. Høglund, M. O. Thompson and M. J. Aziz, "Experimental test of morphological stability theory for a planar interface during rapid solidification," *Phys. Rev. B* **58**, 189 (1998).
24. T.G. Kim, J. M. Warrender and M. J. Aziz, "Strong sub-bandgap infrared absorption in Si supersaturated with sulfur," *Appl. Phys. Lett.* **88**, 241902-241904 (2006).
25. M. J. Aziz, "Interface Attachment Kinetics in Alloy Solidification," *Metall. Mater. Trans. A* **27**, 671 (1996); J.A. Kittl, P.G. Sanders, M.J. Aziz, D.P. Brunco, and M.O. Thompson, "Complete Experimental Test for Kinetic Models of Rapid Alloy Solidification," *Acta Mater.* **48**, 4797 (2000).
26. S. M. Sze, *Physics of semiconductor devices*, 2nd ed. (Wiley and Sons, New York, 1981), p. 69.
27. M. Tabbal, T. Kim, J.M. Warrender, M. J. Aziz, B. L. Cardozo and R. S. Goldman, Unpublished.
28. T. G. Brown and D. G. Hall, "Optical emission at 1.32  $\mu\text{m}$  from sulfur-doped crystalline Si," *Appl. Phys. Lett.* **49**, 245-247 (1986).
29. P. W. Mason, H. J. Sun, B. Ittermann, S. S. Ostapenko, G. D. Watkins, L. Jeyanathan, M. Singh, G. Davies and E. C. Lightowers, "Sulfur-related metastable luminescence center in Si," *Phys. Rev. B*, **58**, 7007-7019 (1998).
30. T. G. Brown, P. L. Bradfield and D. G. Hall, "Concentration dependence of optical emission from sulfur-doped crystalline Si," *Appl. Phys. Lett.* **51**, 1585-1587 (1987).
31. S. M. Sze, *Physics of semiconductor devices*, 2nd ed. (Wiley and Sons, New York, 1981), p. 145.
32. V. Kveder, M. Badylevich, E. Steinman, A. Izotov, M. Seibt and W. Schröter, "Room-temperature silicon light-emitting diodes based on dislocation luminescence," *Appl. Phys. Lett.* **84**, 2106-2108 (2004).

---

## 1. Introduction

Significant effort has been devoted to the development of light emitters based on Si. However, because Si is an indirect bandgap semiconductor, it still remains a challenge to create an efficient Si light-emitting diode (LED) [1]. Si-based LEDs emitting near and above the band gap have been extensively investigated [2-6]. Sub-bandgap LEDs have also been reported mostly using deep-level impurities [8-10] as light-emitting "centers", with some reports of emission from line defects such as dislocations [7]. Such sub-bandgap emission in silicon is particularly important to address the wavelength range of optical communications in a way compatible with on-chip silicon electronics [1]. Optically pumped lasing has been reported [11-13], but an electrically driven silicon laser remains elusive.

In this paper we present a new approach to sub-bandgap light emitting diodes in silicon based on point defect engineering. Our method represents an alternative to the introduction of deep-level impurities or line defects. The control and utilization of point defects that enhance radiative recombination represents a new approach toward creating Si in a stable, optically active form for Si-based optoelectronics [1]. Our materials processing technique, combining ion implantation and pulsed laser melting (PLM), permits the fabrication and retention of high concentrations of optically active point defects and is compatible with existing silicon technology.

## 2. Sample fabrication and experimental results

The emission from our Si LED at wavelength  $\lambda = 1.218 \mu\text{m}$  is a narrow line originating from a direct electronic transition, i.e. a so-called zero-phonon line, in a complex point defect believed to involve mainly silicon self interstitials resulting from ion implantation [14-22]. The inset of Fig. 1 shows a schematic cross section of the LED, consisting of an optically active region where point defects are concentrated, an  $n^+$  top layer and a p-type substrate. Our device was fabricated on a Si(001) p-type (5  $\Omega\cdot\text{cm}$ ) wafer, which was ion implanted at 77 K with 80 keV  $^{28}\text{Si}^+$  to a dose of  $10^{15}/\text{cm}^2$  and subsequently with 80 keV  $^{34}\text{S}^+$  to a dose of  $10^{14}/\text{cm}^2$ . All implantations were carried out at  $7^\circ$  from normal to avoid channeling effects. Samples were subsequently irradiated by a single  $1.4 \text{ J}/\text{cm}^2$  pulse from a spatially homogenized pulsed  $\text{XeCl}^+$  excimer laser (308 nm wavelength, 25 ns full width at half maximum, 50 ns total pulse duration). A  $2.8 \mu\text{m}$  deep,  $120 \mu\text{m} \times 3 \text{ mm}$  ridge structure was then defined on the wafer by photolithography, reactive ion etching and mechanical cleaving. The metallic contacts (back contact Al, 1500 nm; front contact Ti, 5 nm followed by Au, 100 nm) were fabricated using electron-beam evaporation. Finally, the device was processed with rapid thermal annealing for two minutes at  $275^\circ\text{C}$ .

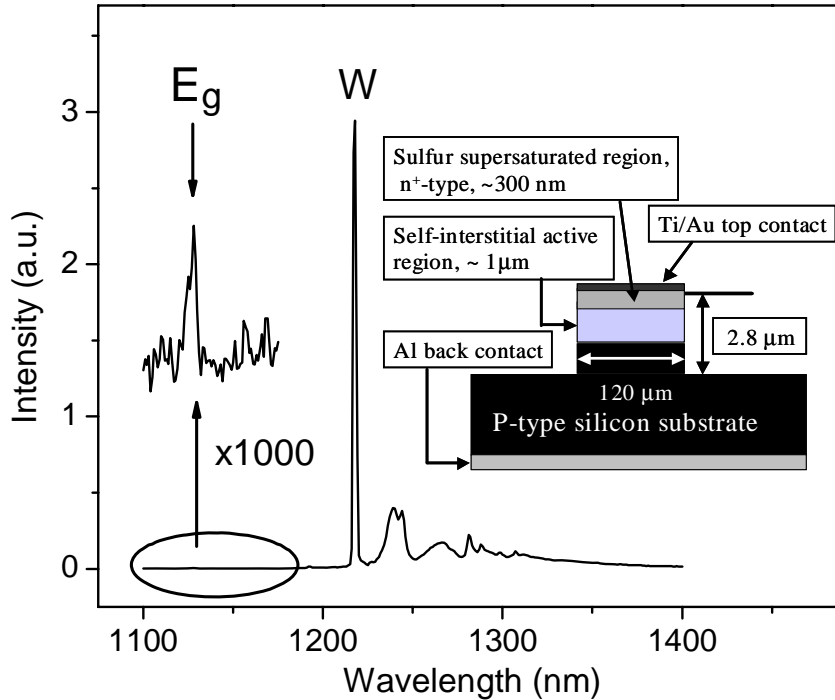


Fig. 1. Surface-emission photoluminescence spectrum of a sample without contacts at 7 K. The inset show the schematic of a Si light emitting diode (not to scale).

The  $1.218 \mu\text{m}$  zero-phonon emission called the W-line [14-20] is commonly observed in irradiated or implanted Si. It is generally understood that clusters of Si self-interstitials are responsible for the W-line emission [14-22], however the exact structure of W-line defects is still under investigation [21,22]. The W-line is initially very weak if it is observed at all from ion implanted Si at low or room temperature. Several methods of thermal treatment have been used to activate W-line luminescence [14-20]. The mechanism for generation and activation of the point defects associated with the W-line appears to be as follows [14-22]. The projected

range (i.e. average depth at which ion implanted sulfur and silicon come to rest) is about 110 nm in our samples, with the concentration of the implanted species dropping well below 0.1% of the peak value by a depth of 300 nm. Many lattice vacancies and self-interstitials (i.e. interstitial Si atoms) are generated along the individual paths of implanted ions due to a number of collisions with the lattice atoms. Some of the Si atoms of the lattice are recoiled well beyond the projected range and come to rest as Si interstitials lacking nearby vacancies with which they can recombine. During thermal annealing, these isolated interstitials migrate and associate to form clusters, e.g. Si bi-interstitials or tri-interstitials.

The ion implantation conditions made the top 160 nm layer amorphous, as confirmed by Rutherford Backscattering Spectrometry in ion channeling mode. During PLM, the laser fluence of  $1.4 \text{ J/cm}^2$  was chosen such that the melt front penetrated about 300 nm, as deduced from time-resolved laser reflectometry and heat flow simulations of melting and solidification [23]. This fluence ensured that the melt depth penetrated beyond the initial amorphous layer, causing subsequent rapid epitaxial plane-front solidification of single crystal Si free of extended defects [24,25]. Despite the low solubility [26] of S in Si, PLM induced rapid solidification creates a highly supersaturated solid solution, which provides an adequate  $n^+$  layer [27]. We believe that other donors should also suffice, and we are currently investigating this issue. The interstitials associated with the W-line have been shown to reside within  $\sim 1 \mu\text{m}$  beyond the melted region [14,15,17,18]. This observation is confirmed by our study, in which the measured W-line PL intensity increased after the removal of 200 nm by KOH etching but entirely disappeared after the removal of  $2 \mu\text{m}$ . It is not known whether during PLM the unmelted interstitial-laden region receives a sufficient thermal treatment for the isolated interstitials to migrate to form clusters [18], but we believe that PLM is a particularly advantageous transient thermal processing treatment for fully annealing the near-surface amorphous/heavily damaged region while preserving the deep interstitial-related defects in a form and concentration suitable for the formation of a high density of W-line defects upon subsequent thermal annealing at  $275 \text{ }^\circ\text{C}$ . We have also observed W-line photoluminescence by simply etching away the near-surface amorphous/heavily damaged layer, and we cannot rule out the possibility of forming a p/n junction in such material by some method other than PLM.

Photoluminescence (PL) and electroluminescence (EL) measurements were performed in a continuous flow optical cryostat at various temperatures. The 458 nm line from an argon ion laser was used to optically excite samples, and luminescence was collected and analyzed by a single grating spectrometer equipped with an InGaAs infrared detector.

Figure 1 shows a typical surface-emission PL spectrum of a sample. The sample was prepared identically to the LED samples, except that the deposition of metallic contacts was skipped. The PL spectrum shows a strong W-line at  $1.218 \mu\text{m}$ , as well as its weaker phonon replicas at longer wavelength [14-20]. Previous studies on dilute sulfur doped Si, with concentrations ranging from  $3 \times 10^{15}$  to  $5 \times 10^{17} \text{ S/cm}^3$ , showed sulfur related emission lines near  $1.3 \mu\text{m}$  and  $1.5 \mu\text{m}$  [8,28-30]. Their absence here is probably due to unusually high S concentrations ( $\sim 3 \times 10^{18} \text{ S/cm}^3$ ) in our samples [24], confirming previous reports [30] on the quenching of the sulfur related emission for concentrations exceeding  $10^{17} \text{ S/cm}^3$ .

Current (I) vs. voltage (V) characteristics at room and low temperature are shown in Fig. 2 (right). The I-V curves show a very good rectifying behavior. The increase of turn-on voltage at low temperature is attributed to the high resistance of the p-type substrate due to carrier freeze out effects.

Electroluminescence is obtained from a cleaved edge of the device. Spectra at 6 K and 80 K are shown in Fig. 2 (left). At 80 K, the intensity of the W-line decreases significantly, and a longer wavelength broadband emission starts to appear. Again, sub-bandgap emission related to dilute sulfur is not observed [8].

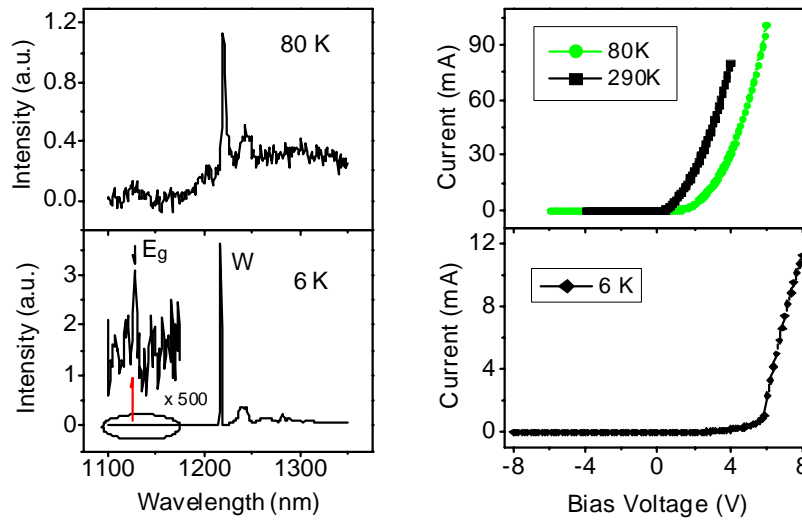


Fig. 2. (right) Current –voltage curves at temperature 290 K, 80 K and 6 K. (left) Edge-emission electroluminescence spectra of the LED at a temperature of 80 K and 6 K. The black arrows indicate the position of the Si band-edge luminescence.

Figure 3 shows the temperature dependent emission intensity of the W-line. The W-line emission starts to drop significantly around 50 K. The linear fit from intensity versus reciprocal temperature gives us its deactivation energy, about 70 meV, which agrees well with the value reported from PL measurements<sup>18</sup>. The emission power of W-line versus injection current at 6 K is shown in the inset of Fig. 3. The intensity increases linearly at currents between 10  $\mu$ A and 4 mA. Above 4 mA, the increase becomes sub-linear. At even larger current than shown, the intensity levels off and eventually decreases, possibly due to reversible heating effects. Our LED characteristics are very stable, showing no evidence of performance degradation after several thermal cycles between cryogenic and room temperature. The measured optical power at a current of 2 mA is about 1.8 nW, which corresponds to an estimated external quantum efficiency  $\sim 10^{-6}$ . This small value results from the poor light collection efficiency ( $\sim 10^{-4}$ - $10^{-5}$ ) associated with the lack of waveguiding from the substrate side and other factors such as low numerical aperture of collection lens and the roughness of the etched ridge and cleavage surface. While a reliable value of the internal quantum efficiency is difficult to determine at this stage, we note that the intensity of the W line is about three orders of magnitude larger than the band-edge luminescence in the same samples. The W-line photoluminescence intensity is about 30 times the band-edge photoluminescence of the virgin substrate, but this comparison is not reliable either, because the absorption of the pump radiation is different in the two specimens.

#### 4. Discussion and summary

Defects are normally associated with problems of device degradation and reliability. They often introduce states in the gap, which, for example, introduce non-radiative recombination in photonic devices through the well-known Shockley-Read-Hall mechanism [31]. Instead, in our device, highly localized point defects are used to create paths of enhanced radiative recombination. Extensive studies have shown that the W-line is a zero phonon line [14-22], which implies that no lattice relaxation is involved. The non-polar nature of optical phonons

in silicon implies that the electrons and holes are not coupled to optical phonons by the Coulomb interaction, unlike in III-V semiconductors. Consequently the role of competing nonradiative channels is reduced.

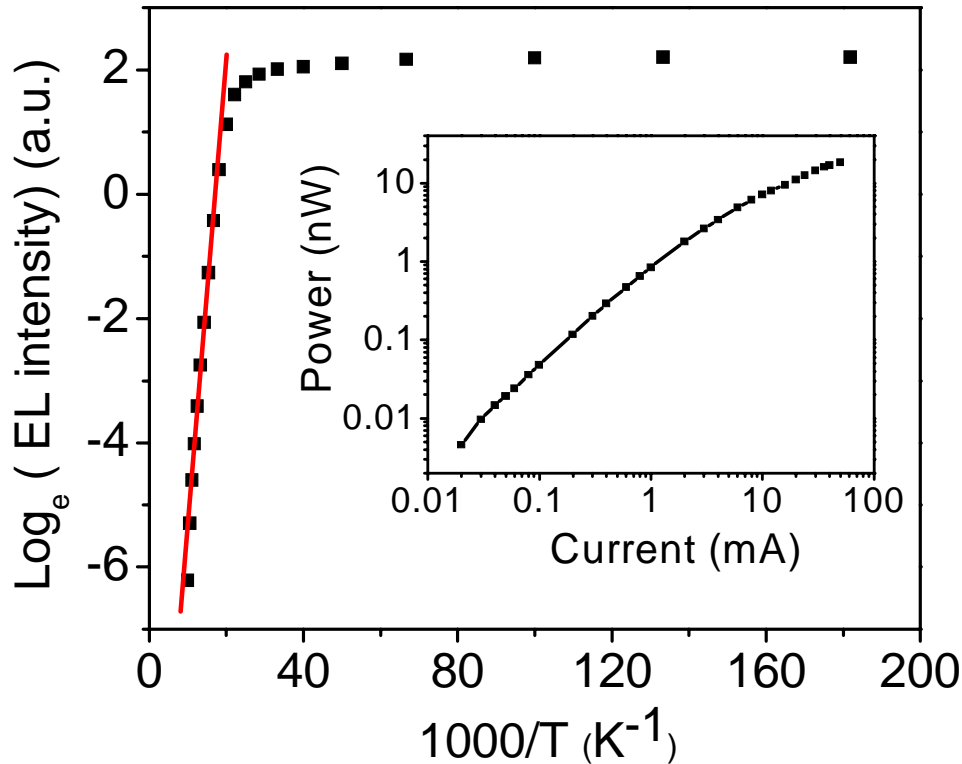


Fig. 3. Temperature dependent intensity of W-line emission at a constant current of 5 mA. The red straight line is the best fit to the high temperature data points. The inset shows the W-line emission power as a function of injection current at 6 K. The line is a guide to the eye.

These results give grounds for optimism about the prospects for substantial improvement in the external quantum efficiency. For example, the defect populations can be engineered through optimized processing. A better optical cavity can be constructed on a silicon-on-insulator (SOI) wafer to reduce optical losses. The most significant drawback of our device is that the W-line emission becomes very weak at higher temperature, vanishing near  $\sim 100$  K. Impurity gettering and hydrogen passivation are known to significantly reduce the temperature quenching of light emission from dislocations in silicon [32]. Additionally, Si point defects show rich spectra. Longer wavelength emission has been observed upon annealing interstitial-rich Si at higher temperature [17,18]. These long wavelength emissions may show a weaker temperature quenching effect due to the deeper level involved in the optical transition and thus might be used to fabricate higher temperature optoelectronic devices.

In summary, we have engineered point defect concentrations in Si for enhanced radiative recombination and thereby demonstrated a sub-bandgap Si LED. Point defects in Si provide a new approach towards Si-based optoelectronic devices.

#### Acknowledgments

We thank Prof. G. D. Watkins, Prof. M. Loncar, Dr. M. Belkin, Dr. L. Diehl, Dr. C. Pflugl, Dr. J. Deng, M. Zimmerler for helpful discussions and C. Madi for assistance in sample

preparation. F.C. and J.M.B acknowledge financial support from the National Science Foundation Nanoscale Science and Engineering Center under contract PHY0017795. The work of M.J.A. was supported by National Science Foundation grant DMR-0306997. The work of M.T. was supported by the Arab Fund Distinguished Scholar Award. The work of T.K. was supported by the Korea Research Foundation Grant funded by the Korean Government (MOEHRD, Basic Research Promotion Fund), KRF-2004-214-C00156. The support of the Center for Nanoscale Systems (CNS) at Harvard University is also gratefully acknowledged. CNS is a member of the National Nanotechnology Infrastructure Network (NNIN). JSW and SC acknowledge the Australian Research Council for financial support.